Large eddy simulation of a boundary layer with concave streamwise curvature

By T. S. Lund

1. Motivation and objectives

One of the most exciting recent developments in the field of large eddy simulation (LES) is the dynamic subgrid-scale model (Germano *et al.* 1991). The dynamic model concept is a general procedure for evaluating model constants by sampling a band of the smallest scales actually resolved in the simulation. To date, the procedure has been used primarily in conjunction with the Smagorinsky (1963) model. The dynamic procedure has the advantage that the value of the model constant need not be specified *a priori*, but rather is calculated as a function of space and time as the simulation progresses. This feature makes the dynamic model especially attractive for flows in complex geometries where it is difficult or impossible to calibrate model constants.

The dynamic model has been highly successful in benchmark tests involving homogeneous and channel flows (*c.f.* Germano *et al.* 1991, Moin *et al.* 1991, Cabot and Moin 1991). Having demonstrated the potential of the dynamic model in these simple flows, the overall direction of the LES effort at CTR has shifted toward an evaluation of the model in more complex situations. The current test cases are basic engineering-type flows for which Reynolds averaged approaches have been unable to model the turbulence to within engineering accuracy. Flows currently under investigation include a backward-facing step, wake behind a circular cylinder, airfoil at high angles of attack, separated flow in a diffuser, and boundary layer over a concave surface. Preliminary results from the backward-facing step (Akselvoll and Moin 1993) and cylinder wake simulations are encouraging. Progress toward the airfoil simulations are discussed by Choi and by Jansen, while preliminary diffuser simulations are discussed by Kaltenbach (all in this volume). The present paper discusses progress on the LES of a boundary layer on a concave surface.

Although the geometry of a concave wall is not very complex, the boundary layer that develops on its surface is difficult to model due to the presence of streamwise Taylor-Görtler vortices. These vortices arise as a result of a centrifugal instability associated with the convex curvature. The vortices are roughly 1/3 of a boundary layer thickness in diameter, alternate in sense of rotation, and are strong enough to induce significant changes in the boundary layer statistics. Owing to their streamwise orientation and alternate sign, the Taylor-Görtler vortices induce alternating bands of flow toward and away from the wall. The induced upwash and downwash motions serve as effective agents to transport streamwise momentum normal to the wall, thereby increasing the skin friction. As evidenced by the 1980 AFOSR-Stanford conference on complex turbulent flows, Reynolds averaged models perform poorly for concave curvature since the Taylor-Görtler vortices are not resolved in

these calculations. Historically the *ad hoc* corrections for the effects of curvature have been unsatisfactory. The objective of this work is to investigate the effectiveness of large eddy simulation and the dynamic subgrid-scale model for this flow.

The simulation targets the experimental data of Barlow and Johnston (1988). This experiment is an ideal test case since a rather complete set of velocity statistics are available for several streamwise stations.

2. Accomplishments

A preliminary large eddy simulation of a boundary layer along a concave surface has been performed. The geometry and flow conditions were close to those studied in the laboratory by Barlow and Johnston (1988). A limited comparison with the experimental data has been undertaken. These items are discussed in more detail below.

2.1 Numerical procedure

The computer code for this work is an adaptation of the code written by Choi and Moin (1993). Boundary conditions have been generalized and the dynamic subgrid-scale model has been added (see Kaltenbach, this volume). The incompressible Navier-Stokes equations are solved in a coordinate space where two directions are curvilinear and the third (spanwise) direction is Cartesian. Spatial derivatives are approximated with second-order finite differences on a staggered mesh. A fully-implicit fractional step algorithm is used for the time advancement.
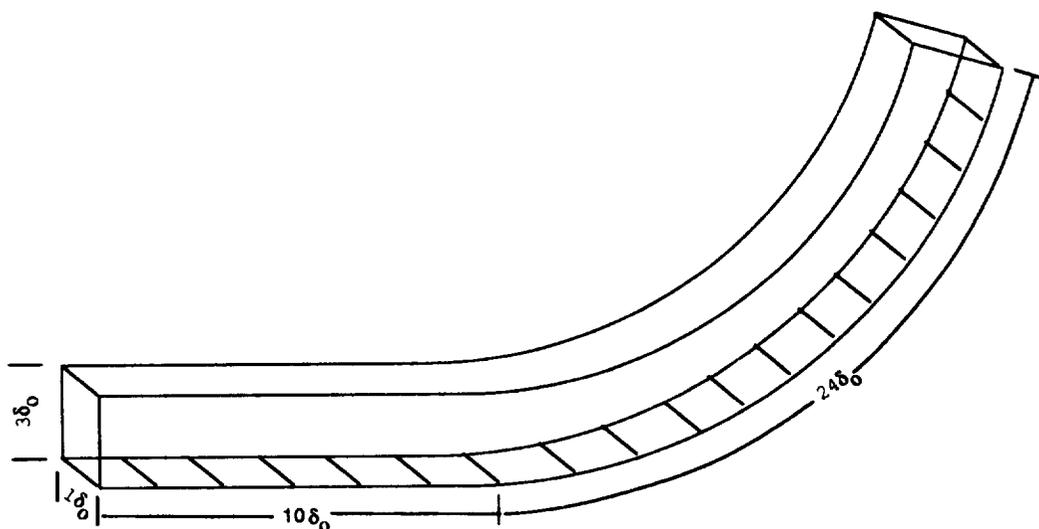

FIGURE 1.   Computational domain. All dimensions are referred to the boundary layer thickness measured at the location where the curvature begins (δ_0). The radius of curvature is $R = 18.1\delta_0$.

Figure 1 shows the geometry for the present simulation. This geometry is similar to that used by Barlow and Johnston (1988) in their experimental study. The boundary layer is allowed to develop along a flat entry section approximately $10\delta_0$ in length, where δ_0 is the boundary layer thickness measured at the location where the curvature begins. At this point the boundary layer encounters a constant radius of curvature bend that turns the flow through 75^0. The ratio of the boundary layer thickness to the radius of curvature, δ_0/R, is 0.055. The domain extends δ_0 in the spanwise direction and $3\delta_0$ in the wall-normal direction. According to the measurements of Barlow and Johnston (1988), the computational domain is just wide enough to enclose one pair of streamwise Taylor-Görtler vortices. Periodic boundary conditions are applied in the spanwise direction while a no-stress condition is applied at the upper boundary. No-slip conditions are applied at the wall. Turbulent boundary layer data from an independent simulation is supplied at the inflow boundary (see Section 2.2 below). A convective boundary condition is applied at the outflow. The computational grid contains $178 \times 40 \times 32$ points in the streamwise, normal, and spanwise directions respectively. The mesh is stretched in the wall-normal direction and uniform in the other two. The grid spacings, based on wall units at the location where the curve begins, are $\Delta x^+ = 98$, $\Delta y^+_{min} = 1$, and $\Delta z^+ = 16$.

The flow conditions match those in the experiment. The momentum thickness Reynolds number at the start of curvature is 1300. The experiment was conducted in water and is therefore incompressible.

2.2 Inflow boundary data

A spatially-evolving simulation such as this one requires the specification of instantaneous turbulent data at the inflow boundary. Although some level of approximation must be made, accurate inflow data is desired to insure minimal transients and realistic turbulence within a short distance downstream of the inlet. Fairly realistic instantaneous inflow data is generated via an auxiliary large eddy simulation of a parallel flow boundary layer. The grid used for the inflow simulation is a truncated version of that used in the main simulation. It extends only one boundary layer thickness in the wall-normal direction and $5\delta_0$ in the streamwise direction. Periodic boundary conditions are applied in the streamwise and spanwise directions, while a no-stress boundary condition is applied at the upper boundary. The inflow simulation is run in parallel with the main simulation in a time-synchronous fashion. At each time step, the velocity field is extracted from the central $y - z$ plane in the inflow simulation. This data is used as the inflow boundary conditions. In practice, the inflow simulation can be either run at the same time as the main simulation or run ahead of time and the inflow data stored on disk. The inflow simulation increases the overall cost of the main simulation by less than 4%.

2.3 Preliminary results

Although the simulation was patterned after the experiment of Barlow and Johnston, there is one important difference in geometry between the two. The experiment

of Barlow and Johnston was conducted in a duct where the boundary layer thickness, δ_0 was about 1/3 of the duct width. The duct was of variable cross-section with the width tailored to minimize the streamwise pressure gradient on the concave wall. The simulation can be viewed as taking place in a constant-width duct where the boundary layer on the convex wall is not present.

Since the simulation was performed in a constant width duct, the boundary layer will experience a streamwise pressure gradient in the vicinity of the onset of curvature. The reason for this is that a normal pressure gradient is required in the curved section to balance the centrifugal force associated with the streamline curvature. The normal pressure gradient requires the pressure to be higher at the concave wall and lower at the convex wall. The development of the normal pressure gradient in the region where the curvature begins induces an adverse pressure gradient along the concave wall. This effect is shown in Figure 2. The pressure is seen to increase abruptly along the concave wall in the vicinity of the onset of curvature. The gradual drop in pressure over the entire length is due to acceleration of the free-stream by the thickening of the boundary layer. Also shown in Figure 2 is the concave wall pressure estimated from the experimentally measured velocity profiles. By virtue of contouring the convex wall, Barlow and Johnston were able to achieve a nearly constant pressure distribution.
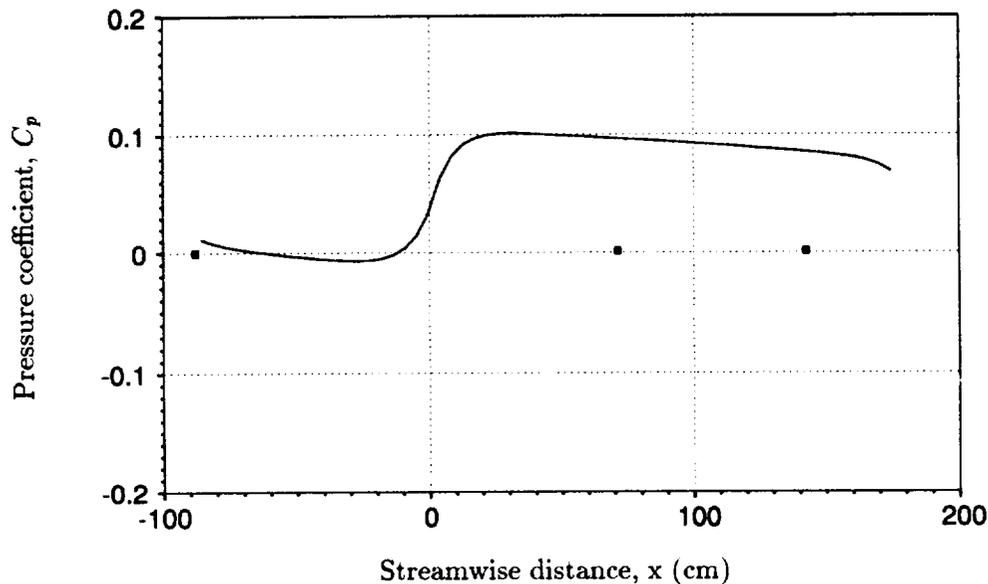

FIGURE 2. Pressure distribution along the concave wall. ——— : simulation; ■ : experiment. The curve begins at $x = 0$.

As discussed below, an inviscid analysis has been performed to determine the location of the streamline in the Barlow and Johnston experiment that lies near the center of the duct. In future simulations this streamline will be used as the upper

boundary where no normal velocity and no stress conditions will be applied. For the present, a rough comparison with the data of Barlow and Johnston can still be made provided that the region affected by the pressure gradient is excluded.
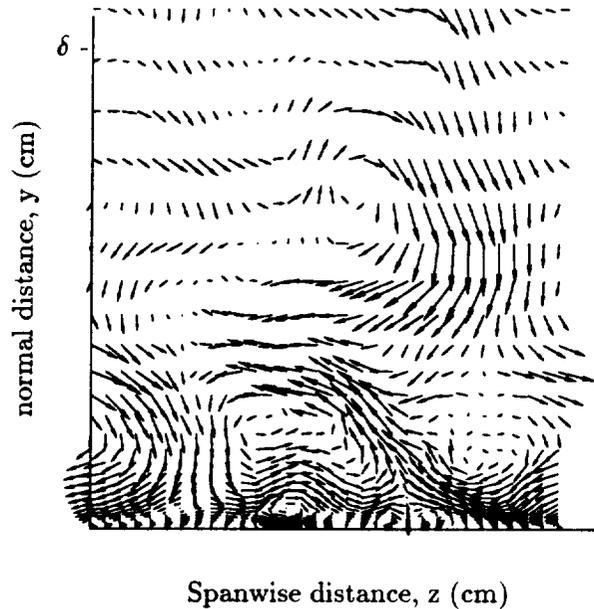

Spanwise distance, z (cm)

FIGURE 3.   Instantaneous velocity vectors in the cross-flow plane at the 60^0 ($x = 142$ cm) station. The label δ indicates the boundary layer thickness.

Instantaneous velocity vectors in the cross-flow plane at the 60^0 ($x = 142$ cm) station are shown in Figure 3. A pair of Taylor-Görtler vortices is evident in the lower 1/3 of the boundary layer. As in the experiment of Barlow and Johnston, the vortices develop a few boundary layer thicknesses downstream of the onset of curvature and are coherent from that point to the 60^0 station. The vortex diameter is about 1/3 of the boundary layer thickness at the 60^0 station. The vortices enhance turbulent mixing near the wall and increase the skin friction as a consequence. This effect is shown in Figure 4 where the skin friction (presented as friction velocity) is plotted as a function of distance along the wall. The curvature begins at $x = 0$. The skin friction initially drops sharply as the boundary layer enters the curve, but this effect is due to the adverse pressure gradient in that region. Following a quick recovery, the skin friction undergoes a monotonic growth with streamwise distance. After the flow has been turned through 30^0 ($x = 71$ cm), the pressure gradient is minimal and the simulation results are expected to differ from the experiment only through history effects. Indeed the simulation results are in reasonable agreement with the experimental data between 30^0 and 60^0. It is also important to note that the skin friction is well behaved near the inflow boundary and does not exhibit a visible transient arising from the approximate turbulent inflow data.
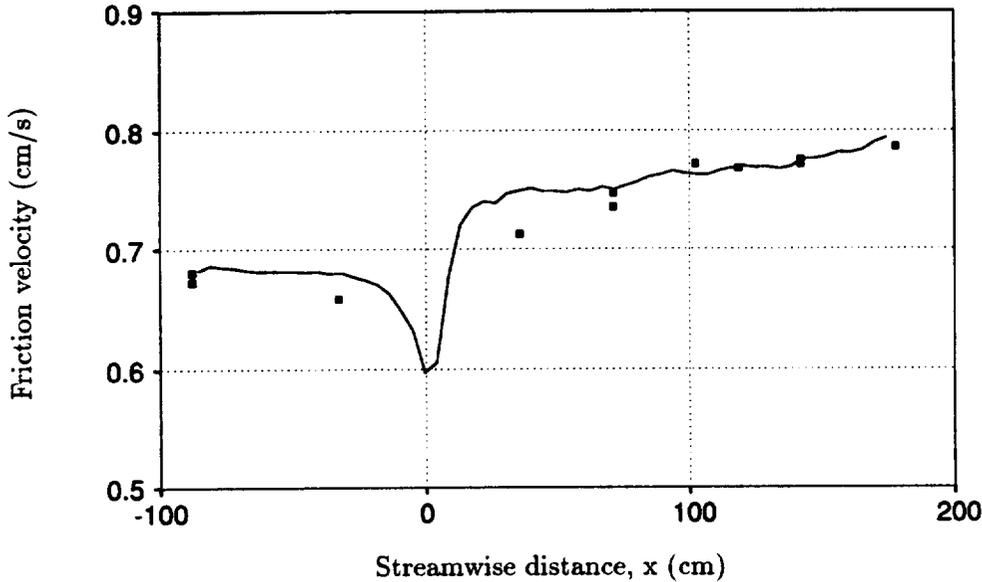
FIGURE 4.   Computed skin friction. ———— : simulation; ■ : experiment. The curvature starts at $x = 0$.

2.4 Streamline for zero pressure gradient

The streamwise pressure gradient discussed above must be removed before a detailed comparison can be made with the experimental data. An obvious way to do this would be to simulate the exact geometry used in the experiment. The drawback of this approach is that the boundary layer on the convex wall would have to be resolved and consequently nearly twice as many grid points would be required. A more economical approach is adopted here where the location of the streamline that lies approximately midway between the two walls of the experimental geometry is determined. This streamline forms the upper boundary in the simulation and results in a pressure distribution very close to that found in the experiment.

The location of the streamline is found using a procedure analogous to that used in designing the experimental facility. An inviscid analysis is used to determine the pressure distribution along the concave wall of a constant-width duct. The shape of the streamline that forms the duct convex wall is then iteratively adjusted in an attempt to minimize the pressure gradient on the concave wall. Once the optimal geometry is determined, the displacement thickness of the boundary layer is estimated and the streamline position adjusted to allow for the thickening of the boundary layer.

Figure 5 shows the streamline determined by the inviscid analysis. The corresponding pressure distribution along the convex wall is shown in Figure 6. For reference, the pressure distribution for a constant-width duct is also shown in Figure 6. It can be seen that the pressure gradient is greatly reduced, but not completely
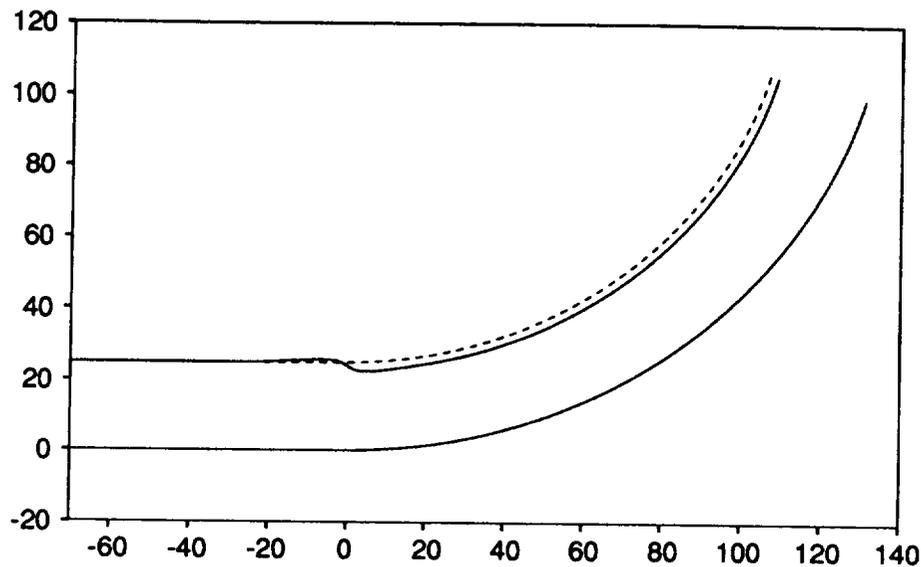
FIGURE 5.   Streamline location for minimization of the pressure gradient at the wall. ——— : streamline; — — — : constant-width reference. Dimensions are in cm.

eliminated. The residual excursions could not be eliminated with a simple algorithm that adjusts the streamline locally in response to the pressure deviation on the opposite side of the duct. Nearly identical pressure excursions are also present in the inviscid analysis used to design the experimental facility. For this reason no attempts were made to further refine the streamline. The boundary layer displacement thickness distribution was estimated from the experimental measurements and the streamline was displaced away from the concave wall accordingly. The final streamline will be used as the upper computational boundary in all future simulations.

3. Future plans

Future work will focus on refining the simulations and in making detailed comparisons with experimental data. The upper boundary location will be changed as described above in order to minimize the streamwise pressure gradient. The mesh spacings will be varied in order to determine the minimal resolution for which acceptable results are obtained. The spanwise extent of the domain will be enlarged so that the spacing of the Taylor-Görtler vortices are not imposed directly. Ideally the spanwise extent should be large enough to support several pairs of vortices. The spanwise length will be made as large as practical given the computer resource constraints. Detailed comparisons will be made between the LES, experimental data, and a simulation run with no subgrid-scale model. The latter will be used to determine the influence of the subgrid-scale model in the overall accuracy of the simulation.
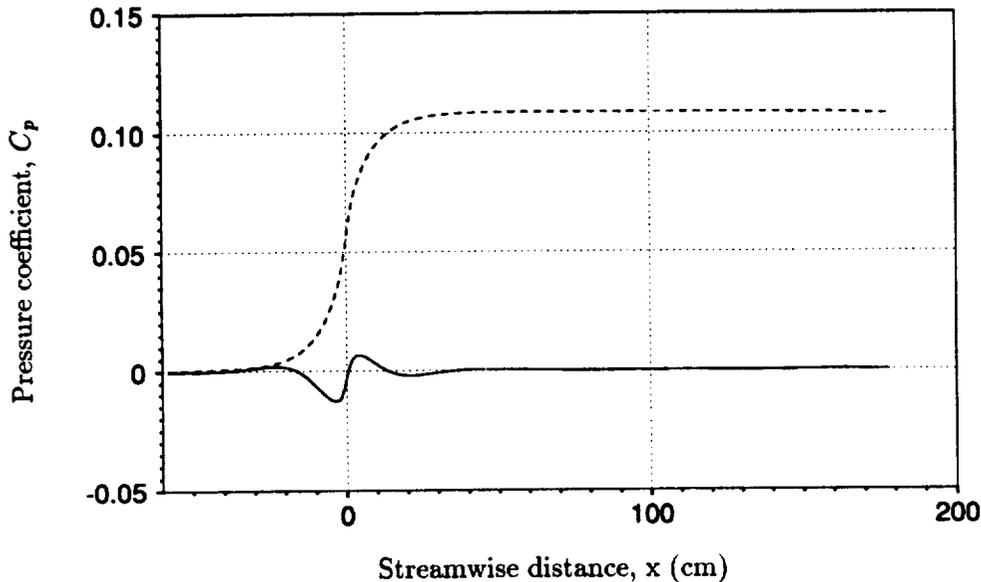
FIGURE 6.   Wall pressure distribution for the streamline shown in Figure 5. ——— : using the streamline boundary; — — — — using a constant-width boundary.

REFERENCES

AKSELVOLL, K. & MOIN, P. 1993 Application of the dynamic localization model to large-eddy simulation of turbulent flow over a backward-facing step. In *Engineering applications of large eddy simulations*, ed. by S. A. Ragab and U. Piomelli. Presented at the ASME fluid engineering conference, Washington D. C. June 20-24, 1993.

BARLOW, R. S. & JOHNSTON, J. P. 1988 Structure of a turbulent boundary layer on a concave surface. *J. Fluid Mech.* **191**, 137-176.

CABOT, W. & MOIN, P. 1993 Large eddy simulation of scalar transport with the dynamic subgrid-scale model. In *Large Eddy Simulation of Complex Engineering and Geophysical Flows*, ed. by B. Galperin. Cambridge University Press.

CHOI, H., & MOIN, P. 1993 The effect of computational timestep on numerical simulation of turbulent flow. to appear in *J. Comp. Phys.* Also published as *Rep. TF-55, Dept. of Mech. Eng.*, Stanford University, 1992.

GERMANO, M., PIOMELLI, U., MOIN, P., & CABOT, W. H. 1991 A dynamic subgrid-scale eddy viscosity model. *Phys. Fluids A.* **3**, 1760-1765.

MOIN, P. SQUIRES, K., CABOT, W., & LEE, S. 1991 A dynamic subgrid-scale model for compressible turbulence and scalar transport. *Phys. Fluids A.* **3**, 2746-2757.

SMAGORINSKY, J. 1963 General circulation experiments with the primitive equations. *Mon. Weather Rev.* **91**, 99-164.